Formation and High Mechanical Strength of Al-Based Alloys Containing a Nanoscale Icosahedral Phase As a Main Constituent

Formation and High Mechanical Strength of Al-Based Alloys Containing a Nanoscale Icosahedral Phase As a Main Constituent*

Akihisa Inoue, Mitsuru Watanabe+, Hisamichi Kimura
and Tsuyoshi Masumoto

Institute for Materials Research

(Received December 28, 1992)

Synopsis

This paper reviews our recent results on the achievement of high tensile strength and good ductility for rapidly solidified Al-Mn-Ln and Al-Cr-Ln (Ln=lanthanide metal) alloys containing an icosahedral phase as a main constituent phase. The good mechanical properties are attributed to the simultaneous achievement of the following three structural effects resulting from rapid solidification and appropriate alloy design; (1) the formation of a mixed structure consisting of nanoscale icosahedral particles surrounded by Al phase, (2) the formation of the icosahedral phase at low solute concentrations, (3) the achievement of an ultra-fine mixed state of icosahedral and approximant regions caused by the phason strain-induced approximant transition in the nanoscale icosahedral particles. The utilization of the structural effects is expected to cause high mechanical strengths combined with good ductility for other quasicrystalline alloys.

I. Introduction

In 1984, Shechtman et al.[1] have discovered that a rapidly solidified $Al_{86}Mn_{14}$ (at%) alloy has a mixed structure consisting of fcc-Al and icosahedral phases. This discovery demonstrates that an icosahedral phase with a five-fold symmetry can exist in a bulk form with a scale of micronmeter. This fact is very striking because the structure cannot be interpreted in the framework of conventional

---

* The 1916th report of Institute for Materials Research.

+ Department of Materials Engineering and Applied Chemistry, Mining College, Akita University, Akita 010, Japan.

crystallography and materials science where all materials consist of either a crystalline structure with two-, three-, four- and six-fold symmetries or an amorphous structure without periodicity on a long-range scale. Thus, the icosahedral structure is different from the crystalline and non-crystalline structures and has been interpreted as a quasicrystal[2] which does not have a periodic atomic configuration on a long range scale and has an orientational order. Consequently, since the discovery of this material, a large number of studies on the alloy systems and compositions where the quasicrystalline phase forms and its structure and properties have been carried out for the last eight years. Important points which have been obtained about quasicrystalline alloys up to date are summarized as follows; (1) the quasicrystalline phase can exist as a thermodynamically stable phase[3,4], in addition to a metastable phase obtained by rapid solidification etc., (2) the stable icosahedral phase is a kind of Hume-Rothery type electronic compound with a constant outer electron concentration[5], (3) the quasicrystalline structure consists mainly of the icosahedral type with a three-dimensional quasi-periodicity and a decagonal type with a two-dimensional quasi-periodicity[6], and (4) the fundamental unit leading to the construction of the icosahedral structure is classified to Mackay and Frank-Kasper types[7]. It has subsequently been clarified that (1) the icosahedral structure consists of an F-type with an ordered quasi-periodicity and a P-type with a disordered quasi-periodicity[8], (2) the preferential growth of the stable icosahedral alloy takes place along the three-fold symmetry and the growth morphology has a pentagonal dodecahedron[4], and (3) the growth of the decagonal phase occurs preferntially along the direction which is perpendicular to the decagonal symmetric plane, namely along the direction with periodic atomic configuration, leading to the growth morphology of decagon[9]. It has further been clarified that the icosahedral phase has the following properties; large values of electrical resistivity[10-12], hardness[13,14] and Young's modulus[15], an extreme brittleness[13], a low coefficient of thermal expansion[16], a significant decrease in the density of electronic state near Fermi surface[17], and an isotropy of Young's modulus without distinct orientation dependence[16]. In addition, when attention is paid to the magnetic property for the quasicrystal, ferrimagnetic icosahedral alloys with large magnetization at room temperature have been discovered[18] in rapidly solidified Al-Pd-Mn-B alloys. The ferrimagnetism has been confirmed to result from the icosahedral structure because the structural transition from icosahedral to crystalline phase causes the disappearance of the ferrimagnetic

properties.

Although the ferrimagnetic icosahedral alloy with large magnetization has recently been found, further development of quasicrystalline alloys seems to be dependent on the point whether or not useful characteristics inherent to the quasicrystalline structure are found. As described above, the icosahedral alloys in Al-based system have larger values of Young's modulus and hardness and a smaller coefficient of thermal expansion as compared with those for conventional Al-based crystalline alloys. Furthermore, these properties are isotropic for the icosahedral alloys. The utilization of these advantages seems to enable the development of a new type of Al-based alloys having high stiffness, high tensile strength and a low coefficient of thermal expansion which cannot be obtained for conventional Al-based crystalline alloys. This paper is intended to review our recent results which have been carried out based on the above-described concept.

II. Possibility for the Formation of Nanoscale Quasicrystalline Alloy in Al-rich Concentration Range

All the quasicrystals reported up to date are extremely brittle and the composition range in which the quasicrystalline phase forms as a main phase is limted to high solute concentration ranges above 15 at%[19]. Furthermore, the grain size of these quasicrystals is usually above 0.5 μm even in the rapidly solidified state. If a mixed structure consisting of quasicrystal as a main phase and fcc-Al phase is formed in an Al-rich composition range and the quasicrystalline phase has a nanoscale grain size, the mixed phase alloy is expected to exhibit good ductility as well as high strength, high stiffness, low coefficient of thermal expansion and good wear resistance which are characteristic for quasicrystals.

As an additional element which has a possibility of producing the above-described fine structure for some Al-based icosahedral alloys[19], we paid attention to lanthanide elements. As the most typical example in which the largest quenching effect was obtained, one can list up the formation of an amorphous phase. The Ln elements including Y are known to be only solute elements leading to the formation of an amorphous phase in Al base binary alloys[20]. Therefore, we examined systematically the microstructure and mechanical properties in a rapidly solidified state for the Al-TM-Ln ternary alloys obtained by adding Ln elements to Al-TM (TM=V, Cr, Mo,

Mn or Fe) binary alloys which have been reported[19] to contain the icosahedral phase. As a result, we have found[21] that an icosahedral phase forms as a main phase for the Al-rich alloys containing 93 to 96 %Al and the grain size of the icosahedral phase is as small as about 20 to 100 nm. It has furthermore been found[21] that the Al-rich alloys exhibit good bending ductility, despite that the main phase is composed of the icosahedral phase. In the following sections, the microstructure and mechanical properties of the Al-TM-Ln alloys in the as-quenched and annealed states will be presented in each alloy system and the subsequent possibility as engineering materials will be investigated.

III. Nonoscale Quasicrystalline Phase in Al-Mn-Ce Alloys

Figure 1 shows the compositional dependence of as-quenched structure in the Al-Mn-Ce system, along with the data of bending ductility and the onset temperature of an exothermic reaction (T_x) due to the decomposition of solid solution or amorphous phase. With increasing Mn and Ce contents, the structure changes from an fcc solution to an amorphous phase through mixed states of fcc plus

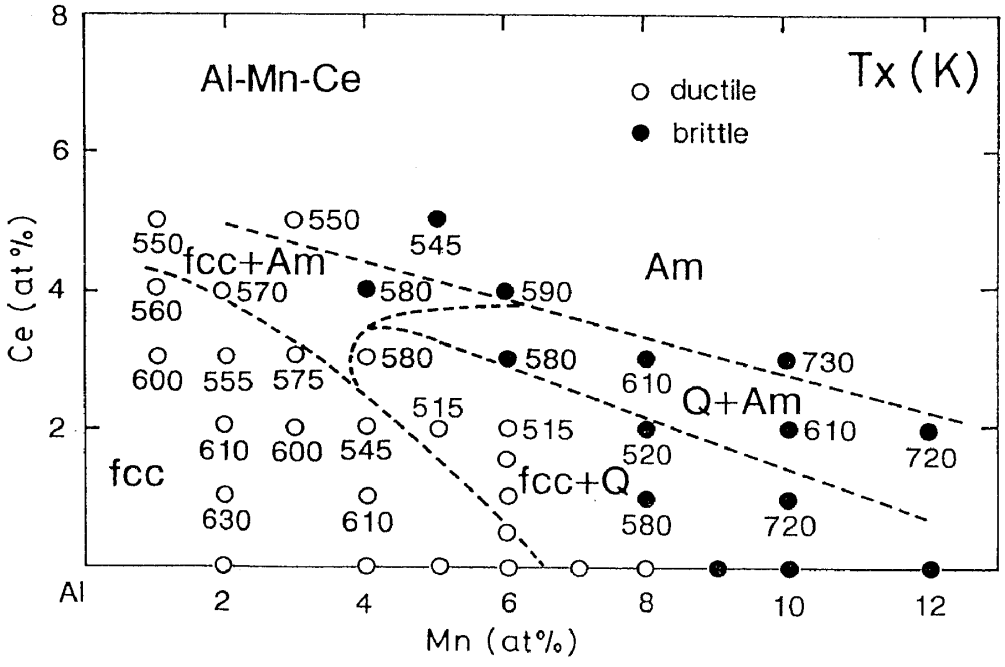

Fig. 1 Compositional dependence of as-quenched phases and decomposition or crystallization temperature (T_x) for rapidly solidified Al-Mn-Ce alloys.

quasicrystalline (icosahedral), fcc plus amorphous and icosahedral plus amorphous phases. Here, it is to be noticed that the icosahedral phase is formed even at the low solute concentrations where the total content of Mn and Ce elements is about 6 %. This indicates that the composition range in which the icosahedral phase forms is extended to a lower Mn concentration range by the addition of Ce. Figure 1 also shows that the ductile alloys which can be bent through 180 degrees are obtained in the Al base solid solution and the coexistent Al and icosahedral phases. Thus, the Ce-containing alloys have a good ductility even in the coexistent state with icosahedral phase. Besides, as shown in Fig. 1, T_x in the fcc phase field tends to decrease with increasing solute content presumably because the metastability of the fcc supersaturated solution decreases with increasing the degree of the supersaturation. On the other hand, there is a clear tendency for T_x in the coexistent amorphous and fcc or quasicrystalline phase field to increase with increasing Mn and Ce contents because of the increase in the numbers of the attractive bonding among the constituent elements (Al-Mn, Al-Ce and Mn-Ce pairs) which has been thought[22] to be a dominant factor for the thermal stability of Al-based amorphous alloys.

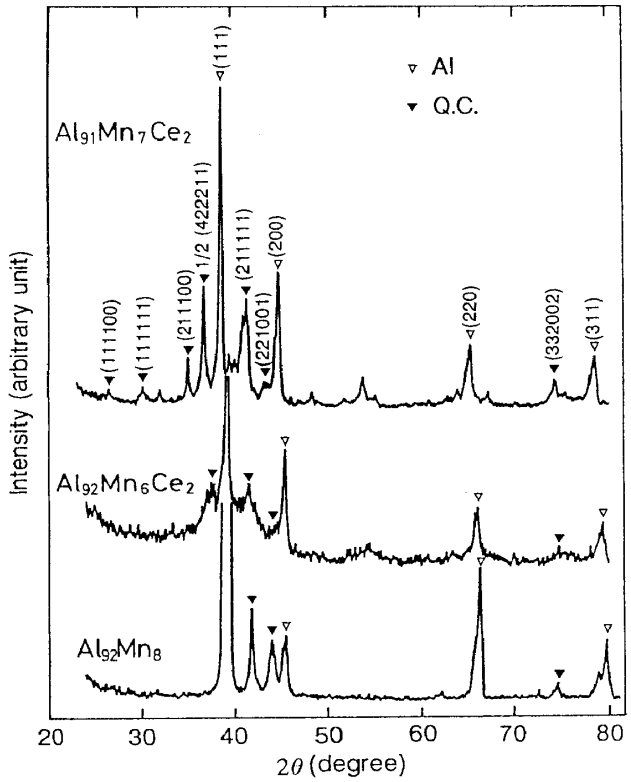

Fig. 2
X-ray diffraction patterns of rapidly solidified $Al_{92}Mn_8$, $Al_{92}Mn_6Ce_2$ and $Al_{91}Mn_7Ce_2$ alloys.

The microstructure of the icosahedral phase in the lower solute concentration range was examined by X-ray diffractometry and transmission electron microscopy. Figure 2 shows the X-ray diffraction patterns taken from the rapidly solidified $Al_{92}Mn_6Ce_2$ and $Al_{91}Mn_7Ce_2$ alloys, along with the data of a rapidly solidified $Al_{92}Mn_8$ alloy. The X-ray diffraction peaks except those of Al phase agree with those of the icosahedral quasicrystal in the Al-Mn alloy and hence the quasicrystalline phase also exists in these Al-Mn-Ce alloys. The diffraction peaks corresponding to the icosahedral phase in the $Al_{92}Mn_6Ce_2$ alloy are rather broad, indicating that the icosahedral phase consists of very fine grain structure and contains a high density of phason defects. Figure 3 shows the bright-field electron micrographs and selected-area diffraction patterns of rapidly solidified $Al_{93}Mn_4Ce_3$ and $Al_{92}Mn_6Ce_2$ alloys with good bending ductility. The as-quenched structure of both alloys consists of equiaxed icosahedral grains of 50 to 100 nm surrounded by an Al phase with a width of 5 to 15 nm. As identified in Fig. 3 (b) abd (d) which are selected area diffraction patterns taken from the circular regions with a diameter of 300 nm, the distinct reflection rings correspond to the icosahedral structure, indicating that the icosahedral equiaxed grains have a random orientation combined with the small grain size. On the other hand, the Al matrix has a fixed crystal orientation on the scale of 300 nm, in spite of the coexistent state with the icosahedral phase. Furthermore, one can notice the significant divergence of the distance between the reflection rings and the 000 reflection spot in the diffraction pattern of the icosahedral phase, indicating that the nanoscale icosahedral particles contain a high density of phason defects as well as some approximant phases.

The confirmation of the unique coexistent structure consisting of equiaxed icosahedral grains and Al boundary phase was also made by dark-field electron microscopy. Figure 4 shows the bright- and dark-field images of the rapidly solidified $Al_{92}Mn_6Ce_2$ alloy. The dark-field image was taken from the reflection rings of $(211111)_i$ and $(221001)_i$. It is clearly seen that only the equiaxed grains show the bright contrast corresponding to the icosahedral reflection rings and no bright-contrast in the grain boundary phase is seen. The equiaxed grains in an isolated state are concluded to be composed of the icosahedral structure. In addition, one can see distinct contrast revealing the existence of a high density of defects in the icosahedral grains, indicating that a large number of phason defects are included in the icosahedral phase.

The solute concentrations in the transgranular icosahedral and

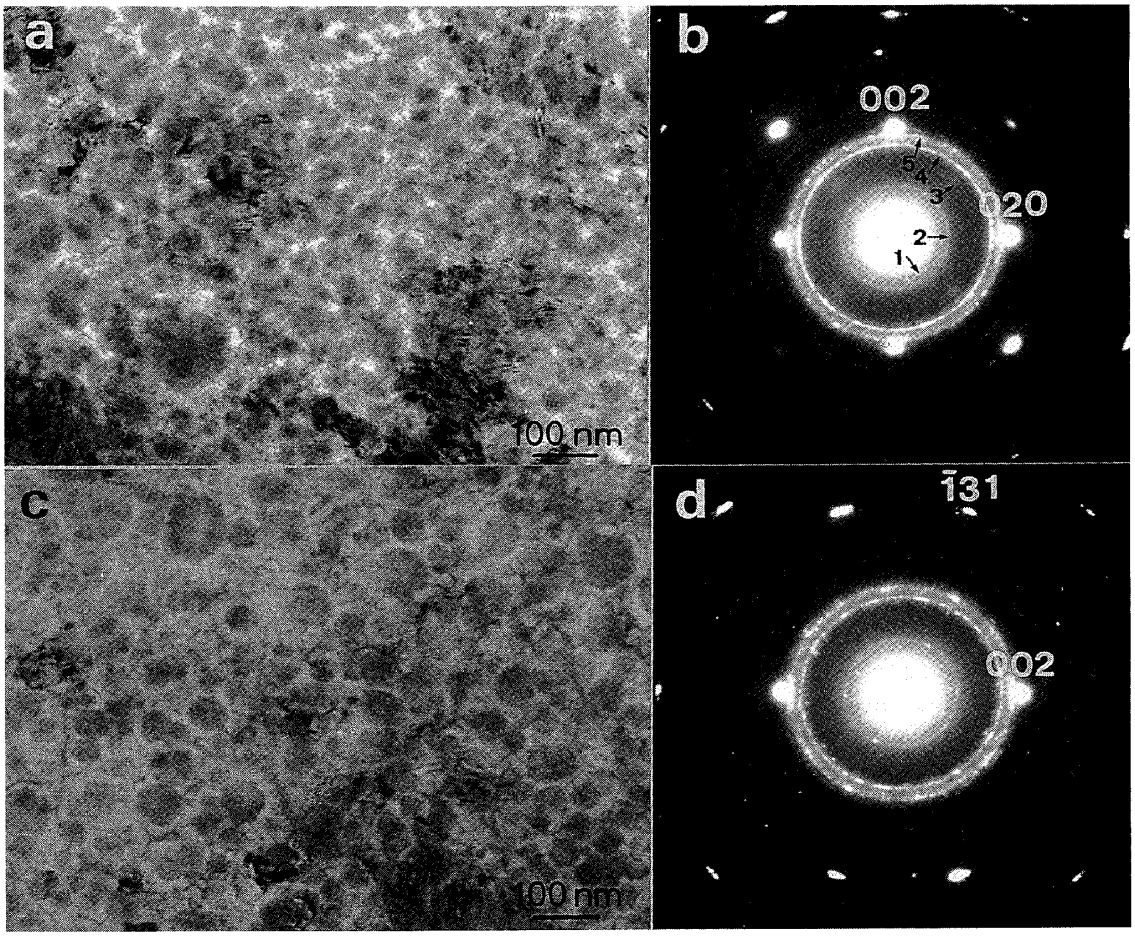

Fig. 3 Bright-field electron micrographs and selected area diffraction patterns of rapidly solidified $Al_{93}Mn_4Ce_3$ (a and b) and $Al_{92}Mn_6Ce_2$ (c and d) alloys. The reflection rings of 1, 2, 3, 4 and 5 in the diffraction pattern (b) are (111000), (111100), (211100), (211111) and (221001) of the icosahedral phase, respectively. The reflection spots indexed in (b) and (d) result from an Al phase and the patterns are identified to be $(100)_{Al}$ and $(310)_{Al}$, respectively.

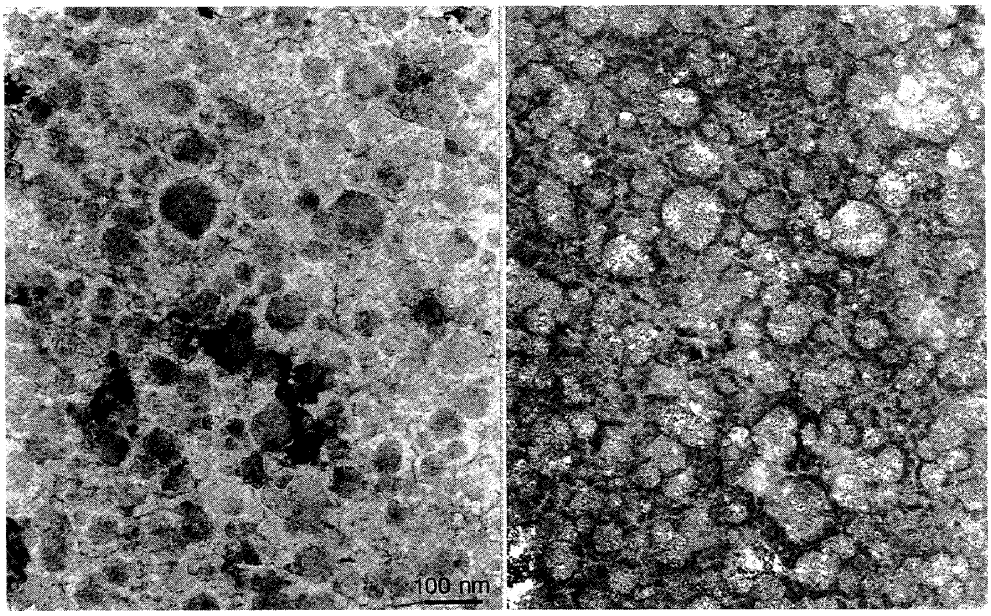

Fig. 4 Bright- and dark-field electron micrographs of a rapidly solidified $Al_{92}Mn_6Ce_2$ alloy. The dark-field image was taken from the $(211111)_i$ and $(221001)_i$ reflection rings of the icosahedral phase.

intergranular Al phase were examined by the EDXS method, in order to determine an approximate concentration of the icosahedral phase in the Al-Mn-Ce alloy. Table 1 summarizes the Al, Mn and Ce compositions of the transgranular icosahedral and the intergranular Al phases obtained by the EDXS method from a limited region smaller than 50 nm in the rapidly solidified $Al_{92}Mn_6Ce_2$ alloy. Additionally, typical examples of the EDXS spectrum taken from the icosahedral spherulite and

Table 1 Energy dispersive X-ray microanalytical concentration of transgranular icosahedral and intergranular Al phase in a rapidly solidified $Al_{92}Mn_6Ce_2$ alloy.

Nominal Composition of Alloy (at%)	Analytical Site	Analytical Mn Concentration (at%)	Analytical Ce Concentration (at%)
$Al_{92}Mn_6Ce_2$	transgranular	7.94	4.36
	intergranular	2.54	1.22

intergranular Al phase in the Al-Mn-Ce alloy are presented in Fig. 5(a) and (b). As seen in Table 1 and Fig. 5, the average Mn and Ce concentrations in the icosahedral phase are about 7.94 at% and 2.54 at%, respectively, and those in the intergranular Al phase are about 4.36 at% and 1.22 at%, respectively. In comparison with the nominal composition ($Al_{92}Mn_6Ce_2$), the Mn and Ce concentrations are higher for the icosahedral phase and lower for the Al phase. However, the solute concentrations of the icosahedral phase are considerably lower than those (18.2 to 22.6 at% Mn)[23] obtained by the same EDXS method for the stoichiometric icosahedral phase in rapidly solidified $Al_{85.7}Mn_{14.3}$ and $Al_{77.5}Mn_{22.5}$ alloys. The significant difference indicates a possibility that the stoichiometric solute concentration of the icosahedral phase shifts to the lower solute concentration side by the dissolution of Ce. However, there is a possibility that the analytical value of the icosahedral phase was obtained from a mixed structure of the icosahedral plus Al phases because of the difficulty in obtaining the information only from an isolated grain resulting from the fine icosahedral grain sizes. Further detailed analysis with a field-emission type TEM will shed some light on the determination of an exact composition of the stoichiometric icosahedral phase in Al-Mn-Ce ternary system. Based on the above-described expermental data,

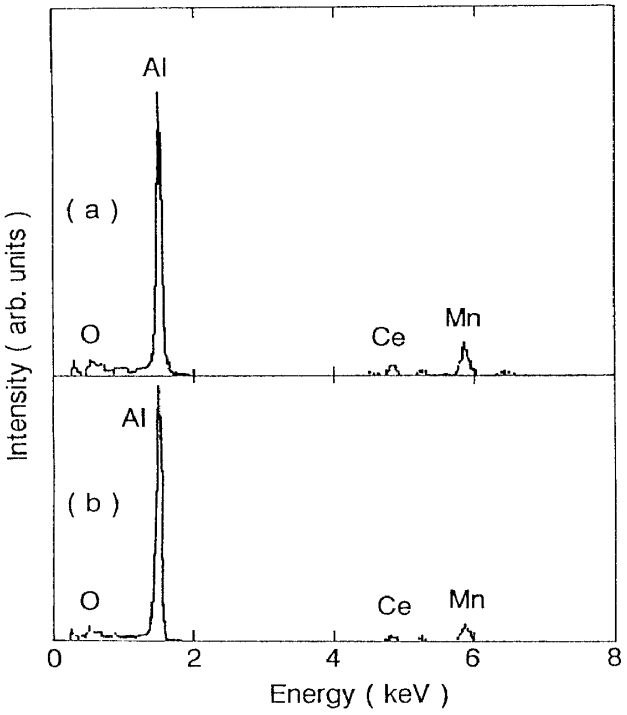

Fig. 5
Energy dispersive X-ray spectra of a rapidly solidified $Al_{92}Mn_6Ce_2$ alloy. (a) Transgranular icosahedral phase, and (b) intergranular Al phase.

such a unique coexistent structure is presumed to be formed through the processes of the precipitation of the primary icosahedral phase and the subsequent solidification of the Al phase from the remaining liquidus phase. The reason why the remaining liquid solidifies as an Al phase is presumably because of the enrichment of the solute elements in the primary icosahedral phase. Here, it should be noticed that the mixed phase alloys have a good bending ductility, in spite of the coexistence of the icosahedral phase as a main phase. The good ductility is also thought to result from the extremely small size of the equiaxed quasicrystalline grains as well as good ductility of the film-like fcc phase which surrounds the icosahedral phase.

It has previously been reported[24,25] that the rapidly solidified $Al_{92}Mn_8$ alloy consists of Al and icosahedal phases and the icosahedral phase has a dendritic morphology characterized by petaline shape with five-fold symmetry. In addition, the grain size of the icosahedral phase is of the order of 0.5 μm. In comparison with the previous data on the icosahedral phase in the Al-Mn binary alloy, it is concluded that the icosahedral phase in the Al-Mn-Ce alloys has a more massive (spherical) morphology and a much smaller grain size. Thus, the addition of a small amount of Ce is very effective for the refinement of the icosahedral grains, accompanied by the spheroidization of the shape through the suppression of the anisotropy of grain growth for the icosahedral phase. Here, it appears important to point out that the Ce element leading to the significant modification of the coexistent icosahedral and Al structure is also effective for the formation of an amorphous phase which can be regarded as an eventual structural modification of the coexistent crystalline structure[26]. The significant structural modification is presumably due to the suppression of atomic diffusivity through the formation of Al-Ce and Mn-Ce pairs with a stronger bonding nature as compared with that for Al-Mn pair. It is to be expected therefore that a similar structural modification is also achieved by the addition of other lanthanide elements.

IV. Mechanical Properties of Nanoscale Quasicrystalline Al-Mn-Ce Alloys

Figure 6 shows the compositional dependence of tensile fracture strength (σ_f) for the coexistent Al plus icosahedral phases and the Al solution with good ductility. σ_f is in the range from 220 to 780 MPa for the Al solution and from 960 to 1320 MPa for the Al plus

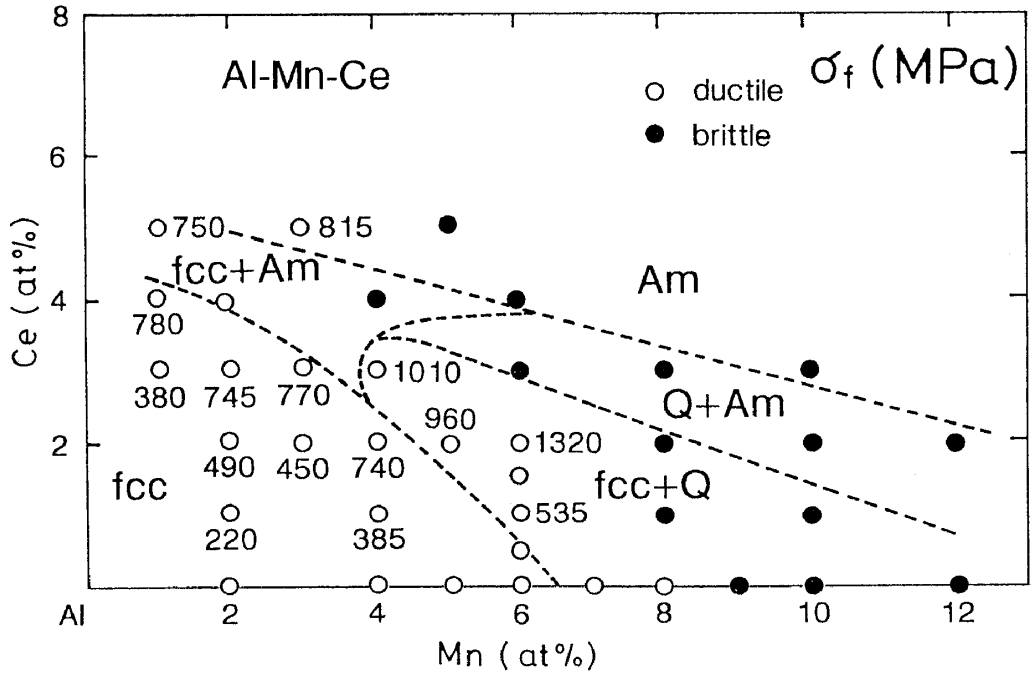

Fig. 6 Compositional dependence of tensile fracture strength (σ_f) for rapidly solidified Al-Mn-Ce alloys.

icosahedral phases. Thus, there is a clear tendency for σ_f to increase with increasing Mn and Ce contents and by the structural change from the Al to the coexistent Al plus icosahedral state. Although the highest σ_f value (780 MPa) for the Al solution is nearly the same as that (860 MPa)[27] for a supersaturated Al solution in the Al-Fe-Ce system, the highest σ_f value of the coexistent Al plus icosahedral phases is much higher than that for the Al solution and comparable to that (1250 MPa)[28] for an amorphous phase in Al-Y-Ni-Co quaternary system. This is believed to be the first evidence for the achievement of σ_f exceeding 1000 MPa at the Al-rich compositions of 92 and 93 at% and in the Al-based alloys containing the quasicrystalline phase as a main phase.

Figure 7 shows the scanning electron micrograph revealing the tensile fracture surface of the $Al_{93}Mn_5Ce_2$ alloy having the coexistent Al plus icosahedral phases. The fracture occurs along the shear plane which is declined by 45 to 50 degrees to the tensile stress direction. The fracture surface consists of a smooth region caused by the shear sliding and a vein region caused by final rupture after the shear sliding. The rather large area fraction of the smooth region indicates that the mixed phase alloy has a good ductility. Furthermore, the distinct ledge pattern is presumed to be formed

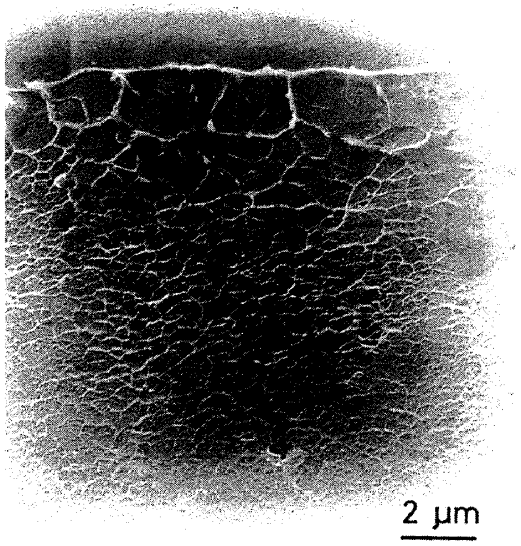

Fig. 7
Scanning electron micrograph showing the tensile fracture surface appearance of a rapidly solidified $Al_{92}Mn_6Ce_2$ alloy.

through the adiabatic final fracture of the Al phase which lies along the grain boundary of the icosahedral phase.

Vickers hardness also shows a similar compositional dependence for the Al solution and the coexistent Al plus icosahedral and Al plus amorphous phases with good bending ductility, as shown in Fig. 8. H_v is in the range of 205 to 400 for the Al solution, 300 to 460 for the

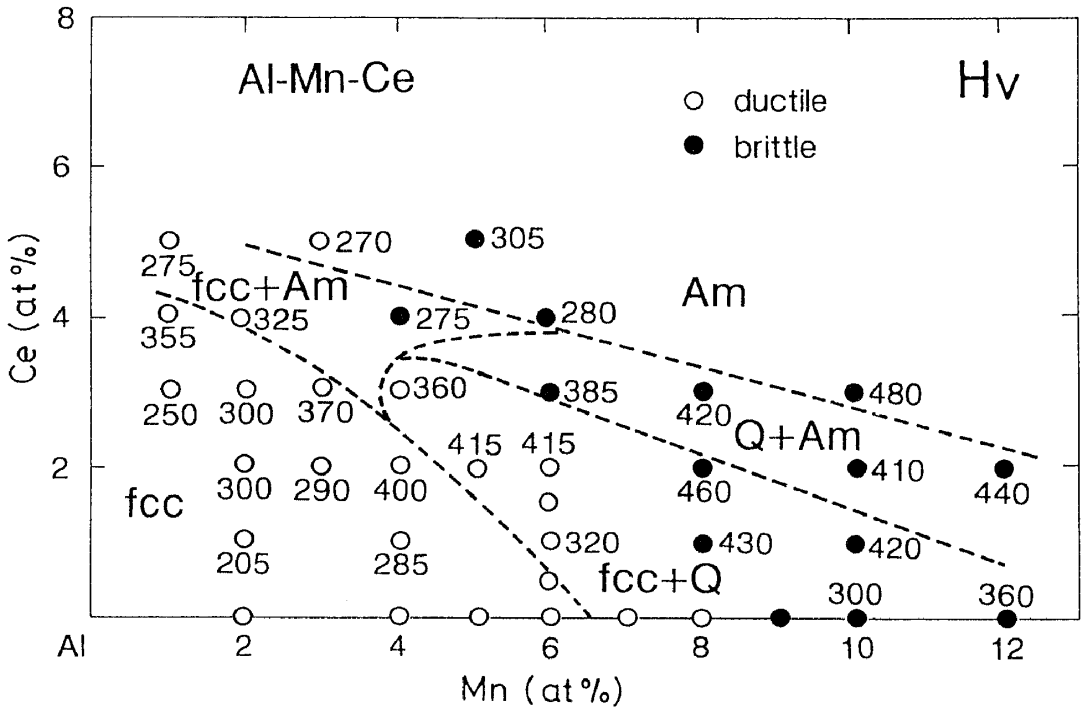

Fig. 8 Compositional dependence of Vickers hardness (H_v) for rapidly solidified Al-Mn-Ce alloys.

Al plus icosahedral phases and 275 to 325 for the Al plus amorphous phases, being considerably higher for the coexistent Al plus icosahedral structure. Furthermore, there is a clear tendency for H_v to increase with increasing Mn and Ce contents.

The coexistent Al and icosahedral phases are in a nonequilibrium state and decompose to an equilibrium mixed structure of Al, Al_6Mn and $Al_{11}Ce_4$ upon subsequent heating[29]. The onset temperature of the phase decomposition (T_x) is about 650 K at a continuous heating rate of 0.67 K/s. Although σ_f of the nonequilibrium phase alloys is kept up to the temperature just below T_x, it decreases significantly by the phase decomposition and σ_f and H_v for the $Al_{92}Mn_6Ce_2$ alloy annealed for 3.6 ks at 573 K are 920 MPa and 450, respectively.

V. Formation and Mechanical Properties of Nanoscale Icosahedral Phase in Al-Mn-Ln Alloys

As described in sections III and IV, the coexistent icosahedral and Al structure in rapidly solidified Al-Mn-Ce alloys is formed in the composition range of 4 to 6 %Mn and 2 to 3 %Ce which is located in the transition region from Al solid solution to amorphous phase and the mixed phase alloys exhibit good bending ductility and high σ_f reaching 1320 MPa. Furthermore, the specific strength defined by the ratio of σ_f to density exceed largely the highest value for Al-based amorphous single phase. It is important for the development of high-strength materials utilizing the icosahedral phase to clarify whether or not coexistent Al plus icosahedral phases with similarly high mehcnaical strengths are formed in Al-Mn base alloys containing Ln elements except Ce by rapid solidification.

Figure 9 shows the X-ray diffraction patterns of rapidly solidified $Al_{92}Mn_6Ln_2$ (Ln=La, Y, Nd or Gd) alloys[29]. As identified for the $Al_{92}Mn_6La_2$ alloy, the as-quenched structure consists of Al and icosahedral phases, in agreement with that for the $Al_{92}Mn_6Ce_2$ alloy shown in Fig. 2. As an example of the microstructure for rapidly solidified $Al_{92}Mn_6Ln_2$ alloys, Fig. 10 shows the bright-field electron micrograph and selected-area diffraction pattern for the $Al_{92}Mn_6La_2$ alloy. As similar for the $Al_{92}Mn_6Ce_2$ alloy, the spherical icosahedral particles with a diameter of about 50 nm exist in an isolated state with an interparticle spacing of about 25 nm in Al matrix. As identified in Fig. 10 (c), the diffraction pattern consists of reflection rings corresponding to the icosahedral phase and reflection spots of Al phase and there is no appreciable crystal orientation

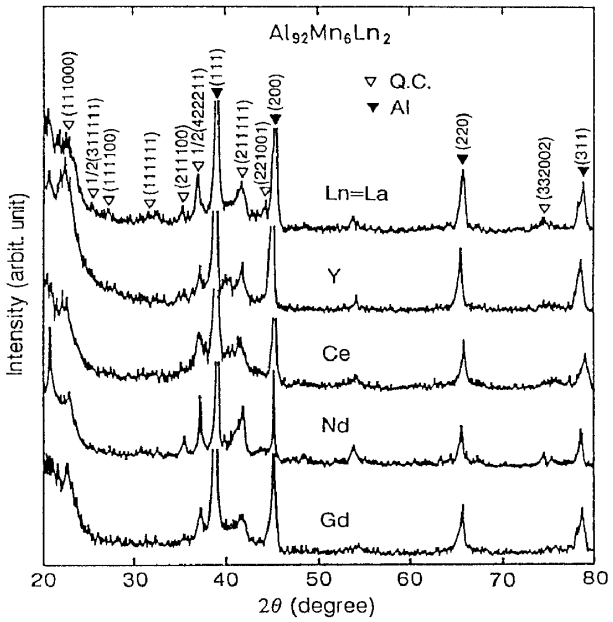

Fig. 9
X-ray diffraction patterns of rapidly solidified $Al_{92}Mn_6Ln_2$ (Ln=La, Y, Ce, Nd or Gd) alloys.

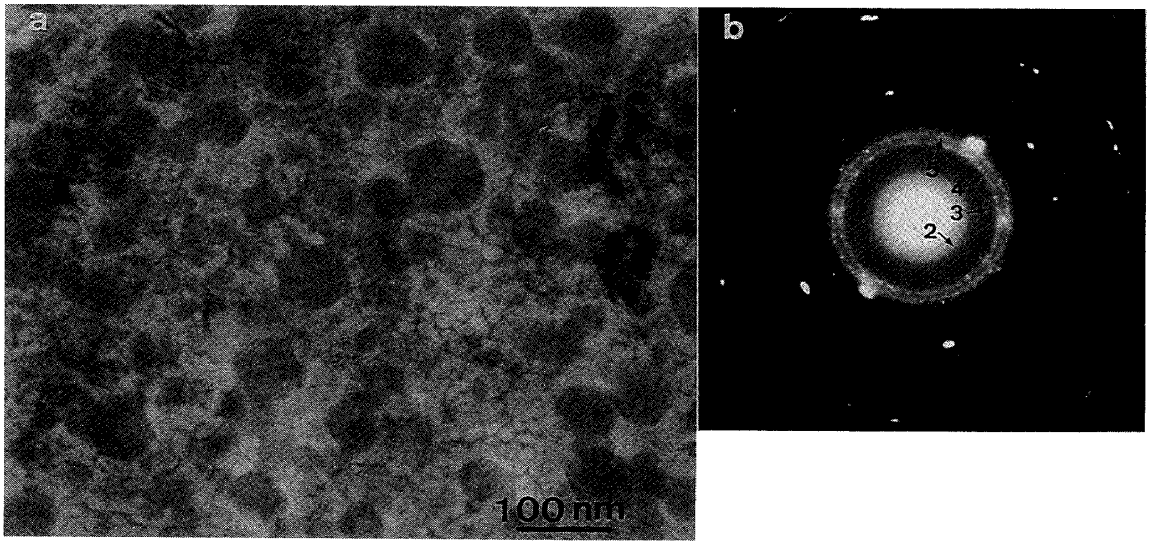

Fig. 10 Bright-field electron micrograph and selected area diffraction pattern of a rapidly solidified $Al_{92}Mn_6La_2$ alloy. The reflection rings of 2, 3, 4 and 5 in (b) are (111100), (211100), (211111) and (221001) of the icosahedral phase, respectively.

between both phases. The similar features in the bright-field image and selected area diffraction pattern are also recognized for the $Al_{92}Mn_6Ln_2$ (Ln=Y or Gd) alloys. All the Al-Mn-Ln alloys having the mixed structure exhibit good bending ductility which is shown by a 180 degree bending and the ductility is independent of the kind of Ln elements.

Figure 11 shows σ_f and H_v for the melt-spun $Al_{92}Mn_6Ln_2$ (Ln=Ce, La, Y, Nd or Gd) ribbons with coexistent Al and icosahedral phases. σ_f exceeds 700 MPa for Ln=Y, Ce, La or Gd, indicating that the formation of the finely mixed structure is effective for the simultaneous achievement of high strength and good ductility. However, σ_f of the Nd-containing alloy is considerably lower than those for the other $Al_{92}Mn_6Ln_2$ alloys. The reason for the lower value for the $Al_{92}Mn_6Nd_2$ alloy was examined by TEM. As a result, it has been reported[29] that the Al-Mn-Nd alloy consists of large icosahedral particles with a size of about 200 nm, in addition to small icosahedral grains with a size of about 20 nm. The morphology of the large icosahedral grains appears to have a petal-like morphology[25,26] inherent to the icosahedral phase in Al-Mn system. This morphology is different from the spherical morphology for the other $Al_{92}Mn_6Ln_2$ alloys exhibiting high σ_f. It is therefore thought that the decrease in σ_f only for

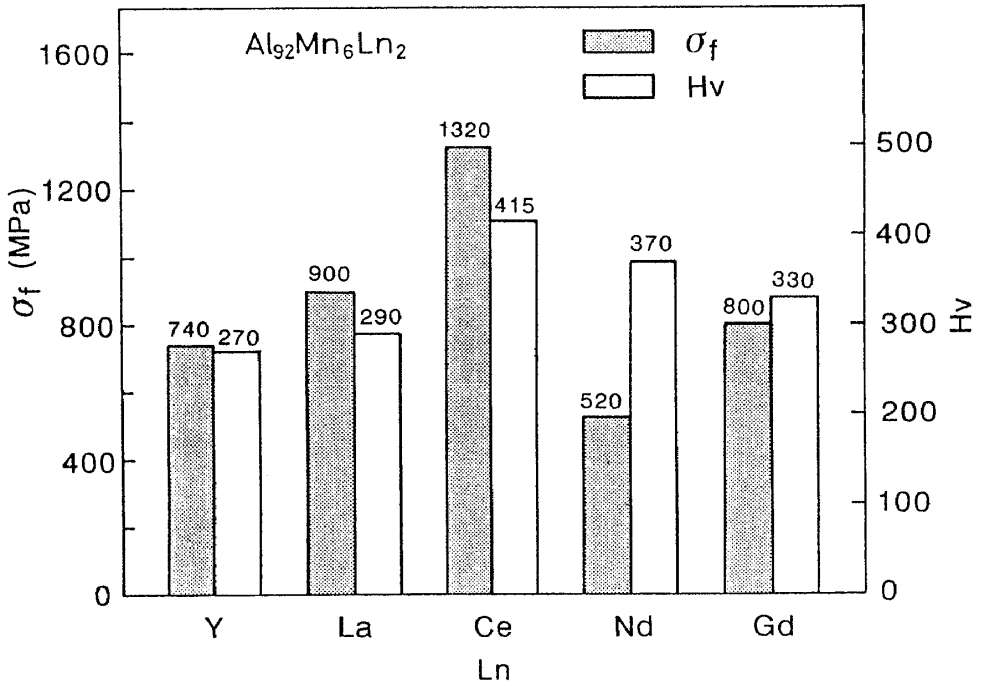

Fig. 11 Tensile fracture strength (σ_f) and Vickers hardness (H_v) for rapidly solidified $Al_{92}Mn_6Ln_2$ (Ln=Y, La, Ce, Nd or Gd) alloys.

the Al-Mn-Nd alloy is due to the significant increase in grain size for the icosahedral phase accompanying the change in the morphology. This result also indicates the importance of grain size of the icosahedral phase for the achievement of high σ_f. However, the reason why the large icosahedral grains form only for the Al-Mn-Nd alloy remains unclear.

VI. Formation and Mechanical Properties of Nanoscale Icosahedral Phase in Al-Cr-Ce Alloys

In sections III to V, we presented the data on the formation of icosahedral plus fcc-Al phases in the rapidly solidified state for the Al-based ternary alloys containing Mn as TM element and the high strength and good ductility of the alloys containing the icosahedral phase as main phase. In the development of high-strength materials by utilizing the nonequilibrium structure, it is very important to clarify whether or not a similar mixed structure consisting of icosahedral plus Al phases forms even in Al-TM-Ln alloys containing TM except Mn and the mixed phase alloys exhibit high tensile strength combined with good bending ductility.

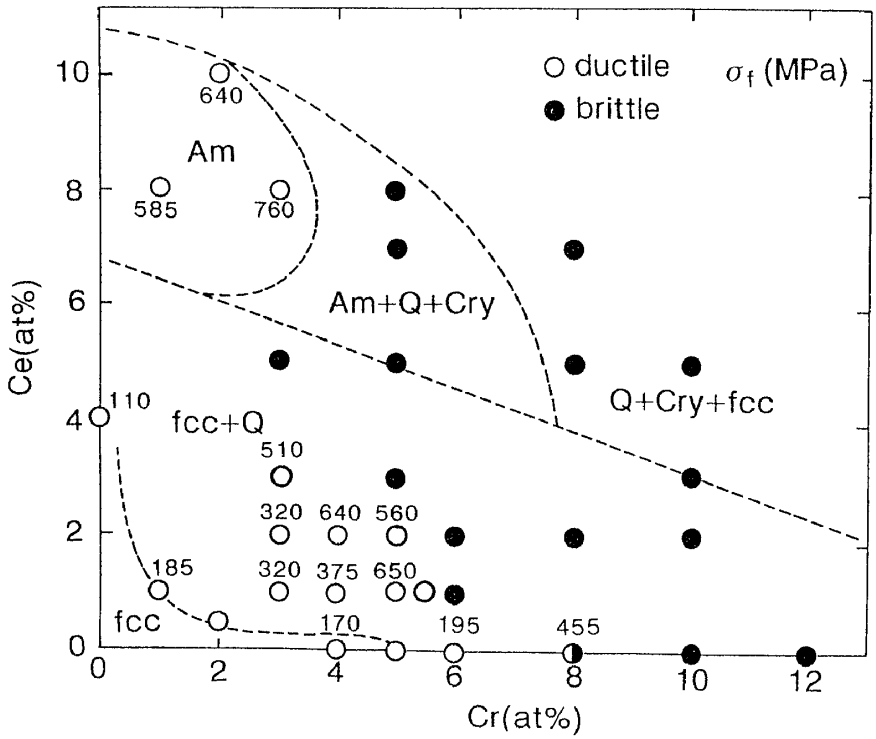

Fig. 12 Compositional dependence of as-quenched phases, ductility and σ_f for rapidly solidified Al-Cr-Ce alloys.

Figure 12 shows the compositional dependence of microstructure and bending ductility for rapidly solidified Al-Cr-Ce alloys[30]. As the solute content (Cr+Ce) increases, the structure changes from Al solid solution to amorphous single phase through the mixed structures of Al plus icosahedral and icosahedral plus amorphous phases. The compositional dependence of the microstructure agrees roughly with that for the Al-Mn-Ce alloys shown in Fig. 1. Figure 12 also shows that the minimum Cr content for the formation of the icosahedral phase decreases significantly by the addition of Ce, indicating that the addition of Ce is effective for the extension of the solute concentration range for the icosahedral phase to a lower solute concentration side. The icosahedral phase in coexistent with fcc-Al has a spherical morphology with a size of about 100 nm and is surrounded by Al phase with a width of about 20 nm, as shown in Fig. 13. The tensile strength of the mixed phase alloy consisting of Al and icosahedral phases also shows a high value of 650 MPa for $Al_{94}Cr_5Ce_1$, as shown in Fig. 12. This strength value exceeds largely the highest strength (550 MPa)[31] for conventional Al-base crystalline alloys. It is therefore concluded that the present strengthening method is also useful for the Al-Cr-Ce alloys.

The formation of a similar mixed structure and the increase in the tensile fracture strength by the existence of the icosahedral phase

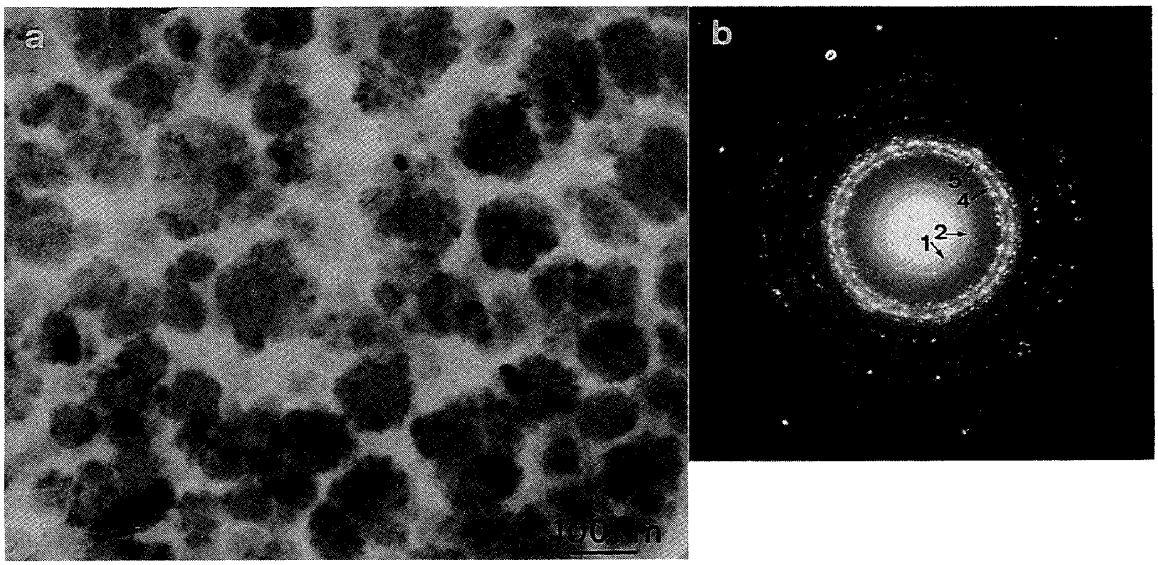

Fig. 13 Bright-field electron micrograph and selected-area diffraction pattern of a rapidly solidified $Al_{94}Cr_5Ce_1$ alloy. The reflection rings of 1, 2, 4 and 5 in the diffraction pattern (b) are (111000), (111100), (211111) and (221001) of the icosahedral phase, respectively.

have also been obtained for rapidly solidified Al-Mo-Ce alloys[32]. These sequent results allow us to conclude that the achievement of high tensile strength combined with good bending ductility through the formation of coexistent icosahedral and Al phases is a universal phenomenon which occurs for all Al-based alloys containing TM elements leading to the formation of icosahedral phase and Ln elements.

VII. The Reasons for the Formation of Icosahedral plus Al Phases and the Increase in Strength and Ductility by the Formation of the Mixed Structure

As shown in Figs. 3, 10 and 13, the icosahedral phase in the coexistent icosahedral plus Al phases has the spherical morphology and the surrounded phase is occupied by Al phase. From the feature of such a structural morphology, it is presumed that the mixed structure is formed through the solidification process of the precipitation of the icosahedral phase containing solute content above the nominal solute content as a primary phase, followed by the formation of an Al solid solution from the remaining liquid. That is, the spherical morphology for the icosahedral phase is presumably because the growth of the icosahedral phase is suppressed by the lowering of temperature due to significant supercooling at the stage before the icosahedral phase has both the faceted growth morphology and a stoichiometric solute concentration after the homogeneous nucleation as a primary phase from liquid. Furthermore, when this solidification process is assumed to be correct, the solidification of the icosahedral and Al phases is complete before the solute concentrations in both the phases attain to the equilibrium state, leading to the absence of a close orientation between icosahedral and Al phases. This presumption is consistent with the present experimental result.

When this concept is appropriate, the grain size of the icosahedral phase decreases and the solute content in the icosahedral phase is lower than the stoichiometric composition of the icosahedral phase and approaches the nominal alloy component with increasing cooling rate. Furthermore, as the difference between the solute concentration in the icosahedral phase and the stoichiometric solute concentration of the icosahedral phase increases, the volume fraction of the icosahedral phase is expected to increase. This is presumed to be the reason for the formation of the mixed structure containing a large amount of icosahedral phase of 50 to 80 vol% even for the alloys with the low solute concentrations. It is reasonable to presume that

the icosahedral phase containing a low solute content has better bending ductility as compared with that for the icosahedral phase with the higher stoichiometric concentration. It is thus presumed that the achievement of significant quenching effect causes the decrease in the solute content in the icosahedral phase combined with the decrease in grain size and the increase in the volume fraction of the icosahedral phase and the simultaneous modification of the as-quenched structure has enabled the achievement of the high tensile strength reaching 1320 MPa for $Al_{92}Mn_6Ce_2$.

At any event, the present structural effect obtained in the nonequilibrium state is concluded to originate from the significant increase in supercooling ability by the addition of Y and Ln elements to the Al-TM alloys. In comparison with the atomic size of Al, that of Y and Ln elements is larger by 21 to 39 %, respectively, while that of the TM elements is also smaller by about 13 %. In addition, the three constituent elements have large negative heats of mixing with each other. It is therefore presumed that the liquid in the Al-TM-Ln system has a highly dense random packed structure and has a high difficulty against the rearrangement of the constituent atoms for nucleation and growth of a crystalline phase. In particular, the diffusivity of Y and Ln atoms with atomic sizes much larger than that of Al is rather low in the supercooled liquid state and the low diffusivity is presumed to enable the formations of the nonequilibrium icosahedral phase with low solute concentrations as well as the amorphous phase.

Although the icosahedral phase has the nanoscale particle size and the low solute concentration, the volume fraction of the icosahedral phase is estimated to be as large as 50 to 80 %. It is therefore thought that the appearance of both high strength and good bending ductility for the mixed phase alloys results from the improvement of the brittleness of the icosahedral phase itself. Here, we shall consider the reason for the improvement of the extreme brittleness for the nanoscale icosahedral particles on the basis of the present experimental data. As shown in Figs. 3,4 and 8, the nanoscale icosahedral particles contain a high density of phason defects. It is well known[33] that the icosahedral phase changes into periodic approximants by the introduction of linear phason defects. Accordingly, it is reasonable to consider that the nanoscale icosahedral phase is composed of icosahedral region and periodic approximant regions on a nanoscale. The coexistence of the two regions is also supported from the result that the micro-micro diffraction pattern obtained from one icosahedral particle using an

objective aperture with a diameter of 7 nm consists of diffuse reflection rings as shown in Fig. 14. There is a high possibility that the periodic approximant phase which is formed in the Al-rich composition range has a rather high plastic deformability. Consequently, the coexistence of ultra-fine approximant phase with the Al-rich concentration seems to be the reason for the simultaneous achievement of high strength and good bending ductility for the

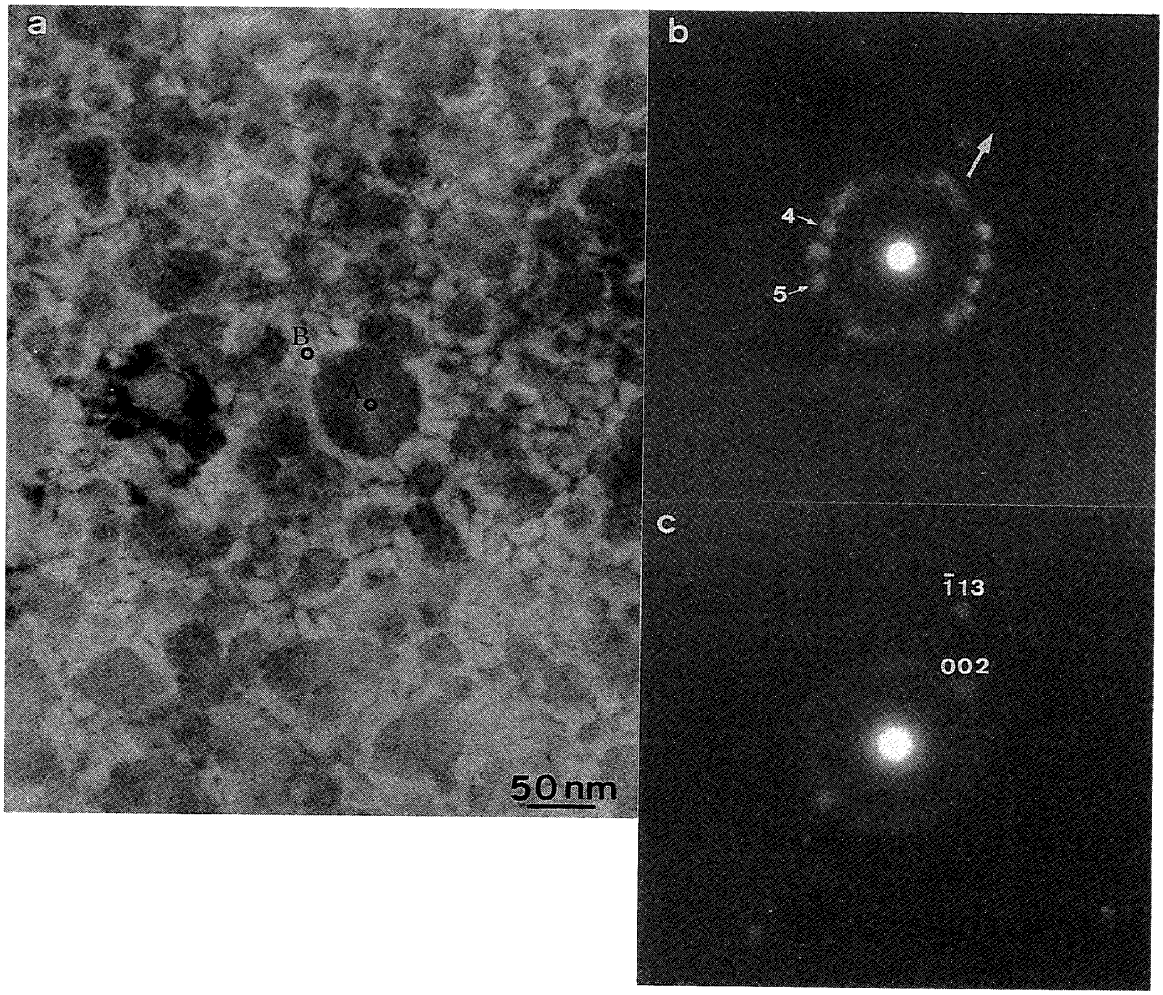

Fig. 14 Bright-field electron micrograph (a) and selected-area diffraction patterns (b and c) of a rapidly solidified $Al_{92}Mn_6Ce_2$ alloy. The patterns (b) and (c) were taken from the regions of the one icosahedral grain marked with A and the Al grain-boundary phase marked with B by using an aperture with a small size of 7 nm. The reflection rings of 4 and 5 in (b) are (211111) and (221001) of the icosahedral phase, respectively, and the diffraction spots indexed in (c) result from an fcc-Al phase.

icosahedral Al-TM-Ln alloys. It is thus concluded that the improvement of the ductility for the icosahedral particles is also due to the formation of periodic approximant phases with ultra-fine sizes caused by the introduction of a high density of linear phason defects, in addition to the refinement of the particle size to the nanoscale and the reduction of the solute concentration in the icosahedral phase. The high density of phason defects are thought to be introduced through the simultaneous achievement of the following factors; (1) the increase in liquid quenching effect by the addition of the Ln elements, (2) the increase in strain resulting from the dissolution of the Ln elements with large atomic size, (3) significant deviation of the alloy component in the icosahedral phase from the stoichiometric composition, and (4) the suppression of the transition into the equilibrium (faceted) growth morphology with a minimum interfacial energy. It is thus said that the Ln elements play an important role in the achievement of the above-described ultra-fine structural modification. Furthermore, it is to be noticed that both the refinement of icosahedral particles to the nanoscale and the introduction of a high density of phason defects under appropriate alloy designs and fabrication processes enable the sub-nanoscale structural control consisting of the icosahedral and periodic approximant phases.

When the icosahedral phase has both the nanoscale grain size and the low solute concentration, why do the tensile strength and bending ductility of the icosahedral phase increase? As the particle size of the icosahedral phase decreases, the thickness of the Al phase between the icosahedral particles also decreases, leading to the refinement of grain size. It is generally known that the refinement of grain sizes in the constituent phases causes the simultaneous increase in the strength and ductility. Furthermore, the decrease in the solute content in the icosahedral phase causes the increase in the fraction of Al-Al pair in the icosahedral phase. As a result, atomic rearrangement so as to relax the stress concentration becomes easy, resulting in the increase in the resistant ability to the nucleation and propagation of cracks.

VIII. Concluding Remarks

It has been believed that the quasicrystalline alloys are extremely brittle and neither high tensile strength nor good ductility is obtained for the alloys containing icosahedral phase as a main

constituent phase. In such a circumstance, it has been demonstrated that the high tensile strength and good ductility for the Al-based alloys consisting mainly of icosahedral phase can be achieved through the simultaneous achievement of the following three factors; (1) the formation of the coexistent icosahedral and Al phases with the nanoscale grain size, (2) the suppression of redistribution of solute elements in the constituent phases to the equilibrium compositions resulting from the increase in the quenching effect, and (3) the formation of periodic approximant phases in the nanoscale icosahedral grains on an extremely fine scale caused by the quenching-induced phason defects. There is a high possibility that an alloy design based on this concept causes the production of new materials. Besides, with the aim of producing bulk materials having the mixed structure of Al plus icosahedral phases, we have also carried out the development of the fabrication processes such as warm extrusion of rapidly solidified powders and high-pressure die casting etc. The progress of these studies is expected to contribute to the increase in the engineering value of the quasicrystalline alloys.

References

1) D. Shechtman, I.A. Blech, D. Gratias and J.W. Cahn, Phys. Rev. Lett., 53 (1984), 1951.
2) D. Levine and P.J. Steinhardt, Phys. Rev., B34 (1986), 596.
3) P. Sainfort and B. Dubost, J. de Phys., 47 (1986), C3-321.
4) A.P. Tsai, A. Inoue and T. Masumoto, Jpn. J. Appl. Phys., 26 (1987), L1505.
5) A.P. Tsai, A. Inoue and T. Masumoto, Mater. Trans., JIM, 30 (1989), 666.
6) L. Bendersky, R.J. Schaefer, F.S. Biancaniello, W.J. Boettinger, M.J. Kaufman and D. Shechtman, Scripta Met., 19 (1985), 909.
7) G.V.S. Sastry, V.V. Rao, P. Ramachandrarao and T.R. Anantharaman, Scripta Met., 20 (1986), 191.
8) S. Ebalard and F. Spaepen, J. Mater. Res., 4 (1989), 39.
9) A.P. Tsai, A. Inoue and T. Masumoto, Mater. Trans., JIM, 30 (1989), 463.
10) K. Kimura, H. Iwahashi, T. Hashimoto and S. Takeuchi, Proc. 3rd Int. Meeting on Quasicrystals, ed. by M.J. Yacaman, D-Romev, V. Castano and A. Gowez, World Scientific, Singapore, (1990), p.532.
11) K. Kimura and S. Takeuchi, Quasicrystals, ed. by P. Steinhardt, World Scientific, Singapore (1991), in press.

12) Y. Yokoyama, T. Miura, A.P. Tsai, A. Inoue and T. Masumoto, Mater. Trans., JIM, 33 (1992), 97.
13) T. Masumoto and A. Inoue, Bulletin Japan Inst. Metals, 25 (1986), 99.
14) S. Takeuchi, H. Iwanaga and T. Shibuya, Jpn. J. Appl. Phys., 30 (1991), 561.
15) T. Koizumi, T. Suzuki, K. Kimura and S. Takeuchi, private communication (March, 1991).
16) Y. Yokoyama, A. Inoue and T. Masumoto, Mater. Trans., JIM, 34 (1993), No.2, in press.
17) J.L. Wagner, B.D. Biggs, K.W. Wong and S.J. Poon, Phys. Rev. B38 (1988), 7436.
18) Y. Yokoyama, A. Inoue and T. Masumoto, Mater. Trans., JIM, 33 (1992), 1012.
19) A. Inoue and A.P. Tsai, Bulletin Japan Inst. Metals, 29 (1990), 782.
20) A. Inoue, T. Zhang, K. Kita and T. Masumoto, Mater. Trans., JIM, 30 (1989), 870.
21) A. Inoue, M. Watanabe, H.M. Kimura, F. Takahashi, A. Nagata and T. Masumoto, Mater. Trans., JIM, 33 (1992), 723.
22) A. Inoue and T. Masumoto, Sci. Rep. RITU, A-35 (1990), 115.
23) A. Inoue, L. Arnberg, N. Lehtinen, M. Oguchi and T. Masumoto, Met. Trans., 17A (1986), 1657.
24) D. Shechtman and I.A. Blech, Mater. Trans., 16A (1985), 1005.
25) K. Hiraga, M. Hirabayashi, A. Inoue and T. Masumoto, Sci. Rep. RITU, A-32 (1985), 309.
26) A. Inoue, K. Ohtera, K. Kita and T. Masumoto, Jpn. J. Appl. Phys., 27 (1988), L1796.
27) A. Inoue, H. Yamaguchi, M. Kikuchi and T. Masumoto, Sci. Rep. RITU, A-35 (1990), 101.
28) A. Inoue, N. Matsumoto and T. Masumoto, Mater. Trans., JIM, 31 (1990), 493.
29) M. Watanabe, A. Inoue, H.M. Kimura, T. Aiba and T. Masumoto, Mater. Trans., JIM, 34 (1993), No.2, in press.
30) H.M. Kimura, E. Oikawa, M. Watanabe, A. Inoue and T. Masumoto, unpublished research (Oct. 1992).
31) Metals Databook, ed. by Japan Inst. Metals, Maruzen, Tokyo (1983), p.176.
32) H.M. Kimura, M. Watanabe, A. Inoue and T. Masumoto, unpublished research (1992).
33) J.E.S. Socolar, T.C. Lubensky and P.J. Steinhardt, Phys. Rev. B34 (1986), 3345.